Accuracy of unmodified Stokes' integration in the R-C-R procedure for geoid computation

Zahra Ismail, Olivier Jamet

Accuracy of unmodified Stokes' integration in the R-C-R procedure for geoid computation

Zahra Ismaïl[1] and Olivier Jamet[2]

[1]École doctorale d'astronomie et d'astrophysique d'Île-de-France (ED127), Paris, France
[2]LAREG, ENSG-Géomatique, IGN, F-77455 Marne-la-Vallée, France

May 20, 2020

Abstract

Geoid determinations by the Remove-Compute-Restore (R-C-R) technique involve the application of Stokes' integral on reduced gravity anomalies. Numerical Stokes' integration produces an error depending on the choice of the integration radius, grid resolution and Stokes' kernel function.

In this work, we aim to evaluate the accuracy of Stokes' integral through a study on synthetic gravitational signals derived from EGM2008 on three different landscape areas with respect to the size of the integration domain and the resolution of the anomaly grid. The influence of the integration radius was studied earlier by several authors. Using real data, they found that the choice of relatively small radii (less than 1°) enables to reach an optimal accuracy. We observe a general behaviour coherent with these earlier studies. On the other hand, we notice that increasing the integration radius up to 2° or 2.5° might bring significantly better results. We also note that, unlike the smallest radius corresponding to a local minimum of the error curve, the optimal radius in the range 0° to 6° depends on the terrain characteristics. We find also that the high frequencies, from degree 600, improve continuously with the integration radius in both semi-mountainous and mountain areas.

Finally, we note that the relative error of the computed geoid heights depends weakly on the anomaly spherical harmonic degree in the range from degree 200 to 2000. It remains greater than 10% for any integration radii up to 6°. This result tends to prove that a one centimetre accuracy cannot be reached in semi-mountainous and mountainous regions with the unmodified Stokes' kernel.

Keywords. Geoid, Remove-Compute-Restore, Stokes' integration, Integration radius, Gravity anomaly grid resolution, EGM2008, GRAVSOFT

1 Introduction

Different approaches for regional geoid and quasi-geoid determination have been proposed, such as least-squares collocation [18, 31], wavelet modeling [22] and the remove-compute-restore (R-C-R) techniques.

In an operational context, one widely used method is the R-C-R procedure along with the Residual Terrain Model (RTM) reduction [2, 17, 26, 31, 29]. This method was introduced by Forsberg [10] in order to combine rigorously the information of three frequency ranges of the gravity field – the short, intermediate and long wavelength signals – through three steps, including a Stokes' integration, to obtain a geoid model.

The precision of the Stokes' integration phase has been studied for long, in particular to investigate the effects of the size of the integration domain, of the computation method and of the improvement brought by modifying the integration kernel itself.

Kearsley (1986) assessed the so-called ring integration method (discrete approximation of the integral) on free-air anomalies by comparing integration results to geoid heights measured as the difference between GPS ellipsoidal heights and levelling on a test network in Ohio, USA [15, 14]. He found that increasing the cap size degraded the evaluation of N, and concluded that the integration radius to compute the contribution of gravimetric data should be in the order of 0.5° for the degree and order of the reference GGM used.

A more detailed study by the same author investigated, within a R-C-R procedure using the OSU81 geopotential model, the relation between the maximum degree n_{max} of the geopotential model and the optimal integration cap size over two test areas in Canada [16]. A strong correlation between $180/n_{max}$ and the optimal cap radius was found, with an optimal cap radius of about 1° for $n_{max} = 180$. He also observed that the choice of the optimum radius was not critical around this value.

In 1998, Higgins et al. compared ring integration to Fourier-based computation of the Stokes' integral in a R-C-R procedure on a data set in Queensland, Australia. They used the EGM96 geopotential model for the removal of low frequencies [12]. They tested for cap sizes up to 1° and found that the optimum was reached for values ranging between 0.2° and 0.5°.

However, some other works, including recent ones, choose larger values of this parameter, ranging from 1° to 3° depending on the terrain characteristics [4, 13, 30].

In this paper, we address the question of the Stokes' integral accuracy from a complementary point of view. Recent satellite missions dedicated to the observation of the Earth's gravity field considerably improved the accuracy and resolution of geopotential models, in particular since the publication of the EGM2008 model complete to degree and order 2159 [23]. This new data gives us the ability to evaluate the computational techniques on synthetic gravimetric data with a reasonably realistic spectral content. The use of synthetic data provides indeed a reference to control the accuracy of the computation process independently of

the gravity data and interpolation quality. A similar approach was adopted for instance by Featherstone [7], using the EGM96 geopotential model, in order to compare the effect of several Stokes' kernel modifications. However, to our knowledge, synthetic experiments were not performed to revisit the question of the Stokes' integration parameters.

The experiments presented here thus intend to study the dependency of the precision of the Stokes' integration on the gravimetric anomalies grid resolution and on the integration cap size, in the ideal situation when the gravimetric data and the reference data are free of any error. They also intend to assess the dependency of this precision to the spectral content of the gravity signal. Gridded gravimetric data as well as reference data are derived from EGM2008 taken as the reference gravitational field. The Stokes' integration study is limited to the unmodified kernel and to a common discretized space-domain integration.

2 Background

The geoid is defined as the equipotential surface of the Earth's gravity field corresponding to the mean sea surface. High-resolution geoid models can be used in numerous applications such as geodesy, geophysics, oceanography, etc. In the last decades, improving the quality of regional geoid models toward a 1 cm accuracy has become one of the major goals of various research groups and mapping agencies [5, 8, 19].

The R-C-R method with RTM reduction [10] combines rigorously the information of three frequency ranges of the gravity field – the short, intermediate and long wavelength signals – through three steps to obtain a geoid model.

1. First, one computes the residual gravity anomalies ($\triangle g_{res}$) – on the geoid in case of geoid computation and on the topography in case of quasi-geoid computation – defined as :

$$\triangle g_{res} = \triangle g - \triangle g_M - \triangle g_{RT} \tag{1}$$

where $\triangle g$ is the free-air gravity anomaly, $\triangle g_M$ is the long wavelength part computed from a global gravity model, $\triangle g_{RT}$ is the short wavelength part computed as the attraction of the residual topography. $\triangle g_{res}$ anomalies are interpolated into a regular grid.

2. The next step is the integration, where the N_{res} geoid or ζ_{res} quasi-geoid residual heights are derived from the residual gravity anomalies through the computation of Stokes' integral. The original Stokes' formula for gravimetric geoid model is given by Stokes [27]:

$$N_{res} = \frac{R}{4\pi\gamma} \iint_{\sigma} S(\Psi) \Delta g_{res} d\sigma \tag{2}$$

where R is the mean Earth radius,γ is the normal gravity on the reference ellipsoid, $d\sigma$ is the integration surface element of the unit sphere and $S(\Psi)$ is Stokes' kernel as function of the spherical distance Ψ between the computation and data point [11].

$$\begin{aligned} S(\Psi) &= \Big\{ \frac{1}{sin(\frac{\Psi}{2})} - 6sin\left(\frac{\Psi}{2}\right) + 1 - 5cos\Psi \\ &\quad - 3cos(\Psi)ln\left(sin\frac{\Psi}{2} + sin^2\frac{\Psi}{2}\right)\Big\} \end{aligned} \tag{3}$$

3. The final step is the "restore" phase, where the long and short wavelengths, which have been removed earlier from the gravity signal, are restored to compute the geoid or quasi-geoid heights.

$$N = N_M + N_{RT} + N_{res} \tag{4}$$

In step 2, Stokes' formula assumes an integration over the whole sphere. For practical considerations, the domain of computation is usually limited to a reduced area around the computation point, and computed on discretized data. Thus, Equation 2 is approximated and evaluated as a limited summation, for $\Psi \leq \Psi_0$, of products of Stokes' kernel and gravity anomalies over a grid, where Ψ_0 is called the integration radius or the integration cap size according to the authors.

Several authors have proposed to modify the Stokes' kernel in order to reduce the truncation error of the remote zone, either in a deterministic way [4] or though a stochastic approach [25], but the unmodified kernel remains in wide use.

In the following, we study the effect of the grid resolution and of the cap size Ψ_0 on the precision of the integration. In section 3, we present the methodology and data used. In section 4 we discuss the experimental results.

3 Methodology and data

3.1 General principles

In order to evaluate the precision of the sole integration step, we use the global gravity field model EGM2008 [23] to generate a set of synthetic data composed of gridded gravity anomalies and reference geoid heights on selected test areas. The low frequencies of EGM2008, up to degree n_{max}, play the part of the geopotential model used in a R-C-R method. The higher frequencies, from degree n_{max} to 2000, play the part of the residual gravity signal.

We consider the case of a quasi-geoid computation. Free-air anomalies are computed on the topographical surface given by a digital terrain model. Since the geopotential model we used has a limited resolution of about10 km, and since we can generate gridded anomalies at any resolution, we did not include,

in our test, a removal of the high frequencies of the gravimetric signal. An error analysis is performed on a set of points chosen within the test areas. In order to observe the effect of the characteristics of the terrain, test areas are of limited size ($1^\circ \times 1^\circ$).

3.2 Test data synthesis and evaluation

Synthesis

More precisely, let us note W_M and g_M respectively as the gravitational potential and acceleration computed from the degrees 0 to n_{max} of EGM2008 (the geopotential model in our experiment), W and g the total potential and acceleration of the considered gravitationnal field given by EGM2008 up to degree and order 2000, and γ the normal acceleration.

For a given $1^\circ \times 1^\circ$ test area, let $\{P_i(\varphi_i, \lambda_i, H_i)\}_{i=1..p}$ be a set of p points, where (φ_i, λ_i) are the geographical coordinates of the point P_i and H_i its normal altitude. Let Q_i be the corresponding point on the telluroid.

The quasi-geoid height ζ_i at point P_i is decomposed into

$$\zeta_i = \zeta_{M,i} + \zeta_{res,i} \tag{5}$$

where $\zeta_{M,i}$ is the contribution of the geopotential W_M and $\zeta_{res,i}$ is the residual quasi-geoid height.

At point P_i, the reference quasi-geoid residual height will be given by the Brun's formula [11]

$$\zeta_{res,i}^{ref} = \frac{W(Q_i) - W_M(Q_i)}{\gamma(Q_i)} \tag{6}$$

The estimated quasi-geoid height $\zeta_{res,i}^{comp}$ is obtained by Stokes' integration of gridded residual anomalies Δg_{res}, computed at each grid point, on the topographical surface given by the DTM, by the spherical approximation of the fundamental equation of geodesy [11]

$$\Delta g_{res} = -\frac{\partial(W - W_M)}{\partial r} - 2\frac{W - W_M}{R} \tag{7}$$

where R is the average radius of the Earth.

The geographical coordinates of the points P_i are randomly chosen within the test area, while their normal altitudes are obtained by a bilinear interpolation in a digital terrain model (DTM) of the area.

The anomaly grids were computed up to 6.5° from the center of each test area. These data sets allow us to test integration radii up to 6°. Although results may be sensitive to larger values of this parameter, 6° is already far beyond the possible values in practice, either because of the computational effort, or because of the lack of gravity data far from the area of interest.

Evaluation

The evaluation of the Stokes' integration results is performed though the comparison between the estimated quasi-geoid heights $\zeta_{res,i}^{comp}$ and their reference values $\zeta_{res,i}^{ref}$. Knowing that Stokes' integration over a limited spherical cap is likely to be biased — since the convolution kernel has no longer a zero mean —, we use the same criterion as Higgins [12] by computing the root mean square error of the differences of quasi-geoid heights along the baselines between every pair of points of the area. For each test area, the precision ϵ of the Stokes' integration is thus evaluated as

$$\epsilon = \sqrt{\frac{2}{p\,(p-1)} \sum_{i=1}^{p-1} \sum_{j=i+1}^{p} \left(\Delta H_{i,j}^{comp} - \Delta H_{i,j}^{ref}\right)^2} \tag{8}$$

where, for computed and reference values

$$\Delta H_{i,j} = \zeta_{res,i} - \zeta_{res,j} \tag{9}$$

Due to the sizes of the zones tested, the baselines taken into account in the computation of the error ϵ range from a few kilometers to about 100 km. We did not separate them into several classes of distance as done in [12], considering that, in the latter study, baselines lesser than 50 km and lesser than 100 km showed a very similar behaviour.

We found that this criterion led to the same conclusions as an evaluation by the standard deviation σ of the difference $\left(\zeta_{res,i}^{comp} - \zeta_{res,i}^{ref}\right)$, and will also use the standard deviation in the following.

3.3 Data and software

As mentioned before, synthetic data are generated using the EGM2008 model [23]. This model can be used for different tasks concerning geoid computation due to its relatively high frequencies and its good fit to the gravity field over different areas [6, 23].
We used the digital model ETOPO5 [1] as a model of the topographical surface considered conventionally as giving the normal heights over the processed areas. We considered that the resolution of 5 arc minutes of the DTM was sufficient with respect to the resolution of the gravity data used.
Stokes' integrals were computed with the *stokes* function of the GRAVSOFT package [28]. Synthetic data are produced by software developed by the authors.

3.4 Test areas

Three different areas were selected in France: a plain, a semi-mountainous and a mountainous area (Figure 1), in order to investigate the effect of the landscape on the choice of the parameters, especially in the case of the mountainous

regions. The accuracy of one centimetre is known to be hard to reach in mountainous areas because of the insufficient gravity data coverage and strong topography signal at short wavelengths [9, 31]. Topography and gravity anomalies are illustrated in Figure 2 and Figure 3. Statistical information on the test areas are displayed in Table 1 and Table 2.

4 Results

4.1 Grid resolution

Since we use the EGM2008 up to degree 2000, a resolution of about 0.1° should be sufficient to represent the content of the gravimetric signal to perform the integration. Therefore, it is expected that the grid resolution will not have much influence over the precision if it is smaller than 0.1°.

This conclusion is confirmed by the experiments. We tested resolutions from 0.005° to 0.5° at a fixed integration radius of 2° and for residual anomalies in several frequency ranges. The value of 2° was chosen in accordance with the results of other experiments (see section 4.2). We decomposed the residual anomalies into frequency ranges in order to test sparse grids fulfilling the requirements of the signal theory.

Figure 4 shows the evolution of the standard deviation of Stoke's integral errors as a function of the grid resolution, averaged on the 3 test areas, and for spherical harmonic degrees from 200 to 2000. Each curve corresponds to a given frequency range and is drawn in the resolution interval allowed by the sampling theory.

For all the frequency ranges, one can observe that choosing a resolution fulfilling strictly the sampling theory (the right extremity of each curve in Figure 4 is not sufficient to ensure an optimal precision. The precision loss at raw grid resolution is likely to come from the numerical accuracy of the integration algorithm. As expected, after a small precision improvement when going toward finer resolutions, the error reaches its minimal value.

All degrees being considered, the degradation of the resolution from 0.005° to 0.075° does not significantly alter the precision. Experiments with other integration radii confirmed these results.

4.2 Integration radius

Findings

Figure 5 shows the error ϵ defined by Equation 8 as a function of the integration radius Ψ_0 for $n_{max} = 199$, (a) for Ψ_0 varying from 0 to 6°, and (b) with a focus on the range 0 to 3°. Our choice to focus the study on the integration of the 200-2000 spherical harmonic degree range was driven by the RCR-RTM context: due to the limits of spatial gravity models and of the residual terrain effect removal, we suppose that the residual anomalies will keep a significant energy in these frequencies. Ψ_0 was sampled at resolution 0.1°, with an oversampling

at resolution 0.01° in the neighbourhood of the first local minimum of the curves.

When averaged on the 3 test areas (Figure 5, continuous curve) the evolution of the error with respect to Ψ_0 shows a general behaviour coherent with previous studies. Kearsley, for instance, already noticed the steep decreasing of the error for small values of Ψ_0, followed by large oscillations [16]. The first minimum of the error occurs for $\Psi_0 = 0.24°$. The absolute minimum of the error is reached for $\Psi_0 = 1.9°$, but with a value of the error smaller than the first minimum by only 7%.

However, this behaviour shows a significant variability according to the area. In the flatter region (Figure 5, Zone 1, dotted curve with the symbol $\times$), the difference between the minimal error ($\epsilon = 0.022$ at $\Psi_0 = 2°$) and the first minimum ($\epsilon = 0.025$ at $\Psi_0 = 0.25°$) is weak. In the semi-mountainous area (Figure 5, Zone 2, dashed line with the symbol +), the curve shows a much poorer precision at $\Psi_0 = 0.25°$ and a real gain to process the integral with an integration radius of 2° (error nearly divided by 3). In mountain (Figure 5, Zone 3, finely dotted line with the symbol ▲), the first minimum is the best choice if one cannot use integration radii larger than 1.5°. However, a much better minimum of ϵ is reached for $\Psi_0 = 2.6°$, with an error decrease of more than 40%. Another fact that must be underlined is that, for all the 3 areas, the error of the integration appears to be very sensitive to the choice of Ψ_0 around the value yielding the best results. Such a behaviour was observed with geopotential models of low degree (up to degree 90) [16], but not at all with models of higher degree.

These findings have some significance regarding operational applications. The precision of the 1st order of the French levelling network is estimated to be $2\ mm/\sqrt{\text{km}}$, meaning that one will expect the rms value of the height differences to be in the order of 2 cm for baselines of 100 km. This value is barely achieved by the best minima on the 3 zones.

Interpretation

Several facts may explain the differences observed with previously published results. The main ones probably concern the data used. Our experiments rely on error-free sets of data. Previous works used real data, with the consequence that both gravimetric data and reference data may be biased. We do not believe that the errors of the reference data play a great part: Kearsley uses for instance an evaluation criterion that eliminates the effects of biases and drifts in the levelling, and more importantly, systematic errors in the GPS heighting [16] . On the contrary, the quality of the gridded anomalies is likely to play a major part. Previous studies rely on gravity measurements with a spacing in the order of 10 km, and an interpolation of this data over a grid – after the removal of the residual terrain contribution for some works.

However, other factors may have to be taken into consideration. First, in

our synthesis of the gravimetric anomalies, we used the spherical approximation of the fundamental equation of geodesy (Equation 7), for which the Stokes' integration is the theoretical solution. With real measurements, anomalies are computed as the difference between the module of the measured acceleration on the topography and the module of the normal acceleration on the telluroid. We verified that the synthetic anomalies from Equation 7 were not biased with respect to anomalies computed from the acceleration modules (rms $\simeq 0.06$ mGal on a $7^\circ \times 7^\circ$ area around our second test area). We thus do not think that this choice influences our results.

Secondly, the results in Figure 5 correspond to $n_{max} = 199$, while other works used different values (180 in [16], and 360 in [12]). The dependency of the optimal radius to the degree of the geopotential model has been well documented as mentioned in section 1. However, this dependency was supposed to be more or less independent of the landscape, and to be characterised by smaller optimal integration radii as the degree of the geopotential model increase. Figure 6 shows the evolution of the error ϵ as function of the integration radius, for the semi-mountainous area and for a few values of n_{max}. The dependency of the location of the first minimum of the curve conforms to the one observed in previous works. One also observes that, as n_{max} increases, the oscillations of the curves become smaller, and nearly fade out for $n_{max} = 360$ (Figure 5, continuous curve with the symbol ●). However, even for this latter value, the integration over a larger domain, up to $\Psi_0 \simeq 2^\circ$, brings some precision improvement.

Finally, the accuracy of the geopotential model itself may be a cause. In our tests, the geopotential model is chosen as the low frequencies of the model used for synthesising the gravity data, which corresponds to an unrealistic situation of perfect removal of the low frequencies. In order to evaluate the possible induced bias, we compared the use of the geopotential models OSU81 [24] and EGM96 [20] at degree and order 180 in place of the low degrees of EGM2008 for the values of W_M in the computation of the residual anomalies (Equation 7). Figure 7 shows this comparison for the three areas. In the plains, and with the OSU81 model (Figure 7, left, dotted curve with the symbol $\times$), we find a behaviour similar to the one observed by Kearsley [16]. The first minimum is reached for $\Psi_0 \simeq 0.3$. Then the error oscillates and grows with the integration radius. However, with EMG96 and EGM2008 (dashed curve with the symbol $+$ and continuous curve with the symbol ▲), while one observes the same oscillations and location of the minima, the error decreases with the radius. This example is interesting since Kearsley's data correspond also to a rather flat area. It tends to show that the improvement of the geopotential models has changed the conditions of use of Stokes' integral in the plain. On the other test areas (Figure 7, center and right), even when using OSU81, there is a significant gain in choosing a larger integration radius, especially in the semi-mountainous area (center). The quality of the geopotential model seems less of a determining factor in those cases.

4.3 Dependency on the spectral content

While the previous experiments bring some information about the behaviour of Stokes' integration, the very error values observed may not be significant. Indeed, the spectral content of the signals we processed corresponds to the full gravity signal in the corresponding spectral bands. In real contexts, this spectral content will vary according to the quality of the geopotential model in the locality of the test areas, and according to the choice made for the removal of the residual terrain effect.

In order to investigate whether general conclusion could be drawn from this study as far as the absolute error value is concerned, we computed the integration on separated spectral bands – defined as intervals of spherical harmonics degrees. Figure 8 shows the dependency of the standard deviation of $\left(\zeta_{res}^{comp} - \zeta_{res}^{ref}\right)$ as function of Ψ_0 to these spectral bands. In the plains (Zone 1), the error is clearly dominated by lowest degrees $(200 - 359)$, with a minimum for $\Psi_0 \simeq 2°$. In the semi-mountainous area (Zone 2), increasing the integration radius from the first minimum does not improve the quality for the lowest degrees $(200 - 359)$. However, it does improve the results for intermediate degrees $(200 - 599;\ 200 - 799)$. In the mountains, the behaviour in much more erratic, but, for $\Psi_0 \geq 1°$, the error is also dominated by the degrees up to 599.

These later spectral ranges are also obviously the ones that model the major part of the energy of the signal, and would be largely modified by a terrain effect removal. The Figure 9 presents the relative precision ε_{rel} of the Stoke's integration values, defined as the ratio between the standard deviation of the error and the standard deviation of the reference signal computed on the test points:

$$\varepsilon_{rel} = \frac{\sigma\left(\zeta_{res,i}^{comp} - \zeta_{res,i}^{ref}\right)}{\sigma\left(\zeta_{res,i}^{ref}\right)} \tag{10}$$

where the standard deviation $\sigma\left(v_i\right)$ of a quantity v_i at the p test points P_i is defined by

$$\sigma\left(v_i\right) = \frac{1}{p}\sum_{i=1}^{p} v_i^2 - \left(\frac{1}{p}\sum_{i=1}^{p} v_i\right)^2$$

One observes that, except for the plain test area, the quality of the estimate of the high frequencies (from degree 600) of the geoid improves continuously with the integration radius. The exception of the plain is not surprising since the energy of the corresponding signal in this area is very low.

Secondly, we note that, from degree 600, the tested spherical harmonic frequency ranges show a similar behaviour, with a relative error keeping between 10% and 20%-25% for all integration radii greater than 1°, with the exception of the degree range 600-799 of the semi-mountainous area. Moreover, disregarding this exception, 10% appears to give a lower bound of the relative error for all the frequency ranges.

This result tends to show that independently of the spectral content of the gravity anomalies or of the geoid, for integration radii lesser than 6°, the precision of the Stoke's integration cannot be better than 10% of the standard deviation of the computed residual geoid.

This gives a basis for a rough estimate of the best achievable accuracy in real cases. For instance, Duquenne [3] provided, in the Auvergne data set, a geoid model covering our second test area, and based on the R-C-R technique using a global gravity field up to 360°. The standard deviation of residual geoid height for this geoid model is about 11 cm. Based on our conclusion, the best accuracy we can expect from a standard Stokes' integration is 1.1 cm, larger values being in fact expected due the other error sources.

5 Conclusion and Recommendations

In order to evaluate the accuracy of integration step in R-C-R procedure, we generated a set of synthetic data based on EGM2008 to degree and order 2000. We studied the influence of the integration radius and of the grid resolution using a standard Stokes' kernel, through an analysis of the accuracy of the computed height differences and of the behaviour the results in different frequency ranges.

As expected, the grid resolution does not affect the results providing that it is kept small enough, as suggested by the sampling theory. Considering the overall errors, the choice of very large integration radii, up to 6°, seems to lack any benefit. Beyond 2° to 2.5°, the precision does not improve significantly. However, the relative precision of the high frequencies (degree > 600) seems to improve gradually with the integration radius for the whole studied interval, suggesting that the local variations of the geoid be potentially better represented with large integration radii. This question would deserve a deeper study dedicated to the evaluation of the accuracy of the height differences along small baselines.

These results partly contradict previous studies led on the basis of real data. First, the choice of relatively small radii (lesser than 1°) does not allow to reach the optimal accuracy on synthetic data. A local minimum of the error is always observed for radii around 0.5° as in previous works. Its very location depends mainly on the degree of the geopotential model as noticed by other authors. Nevertheless, this first local minimum might yield far from optimal results. The choice of the best radius and the gain it brings with respect to the first minimum seems to be highly dependent on the characteristics of the terrain. In addition, the quality of the results appears to be very sensitive to the chosen radius around the optimal location. These findings do not seem to depend significantly on the quality of the geopotential model used to remove the low frequencies of the gravity signal.

These differences with previous works are very likely to come from the lower quality of the gravity anomalies available in real cases. However, this tends to indicate that, with the improvement of the gravity surveying, one has to choose the Stokes' integration radius with caution, possibly by checking the process

results on control data.

Lastly, our results tend to show that, independently of the landscape and from the spectral content of the residual gravity anomalies, the unmodified Stokes' kernel cannot reach a precision better than 10% of the geoid signal to be retrieved. The lower bound of the accuracy is probably even higher since our study does not take into account other error sources, such as the interpolation errors, the spherical approximation errors, the aliasing error, etc.

This work, however, poses new questions. The experiments presented here apply the Stokes' integral to anomalies computed on the topography. Our synthetic data do not in that sense fulfil the strict requirements of the Stokes' theory but should be processed in the frame of Molodensky's theory [21], or at least take into account the effect of the flattening of the ellipsoid.

Moreover, this study was limited to the evaluation of the unmodified Stokes' kernel and on a restricted number of test areas, regardless of the accuracy of the interpolation of the observed gravity anomalies. A similar methodology could be used to evaluate other integration kernels and interpolation methods.

Acknowledgements:

This work was funded by a doctoral scholarship from the University of Tichrine, Latakia, Syria. Figure 1 was drawn with the Generic mapping Tool [ref].

6 Graphics

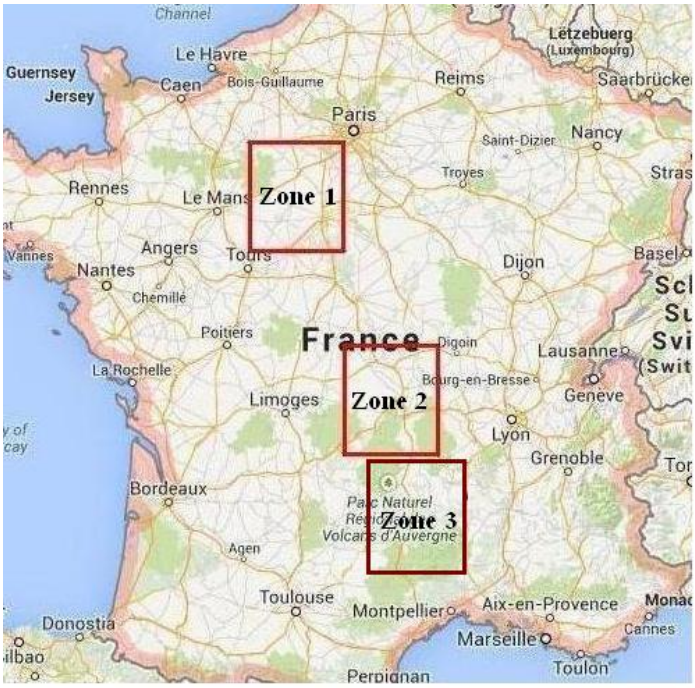

Figure 1: Location of test zones in France

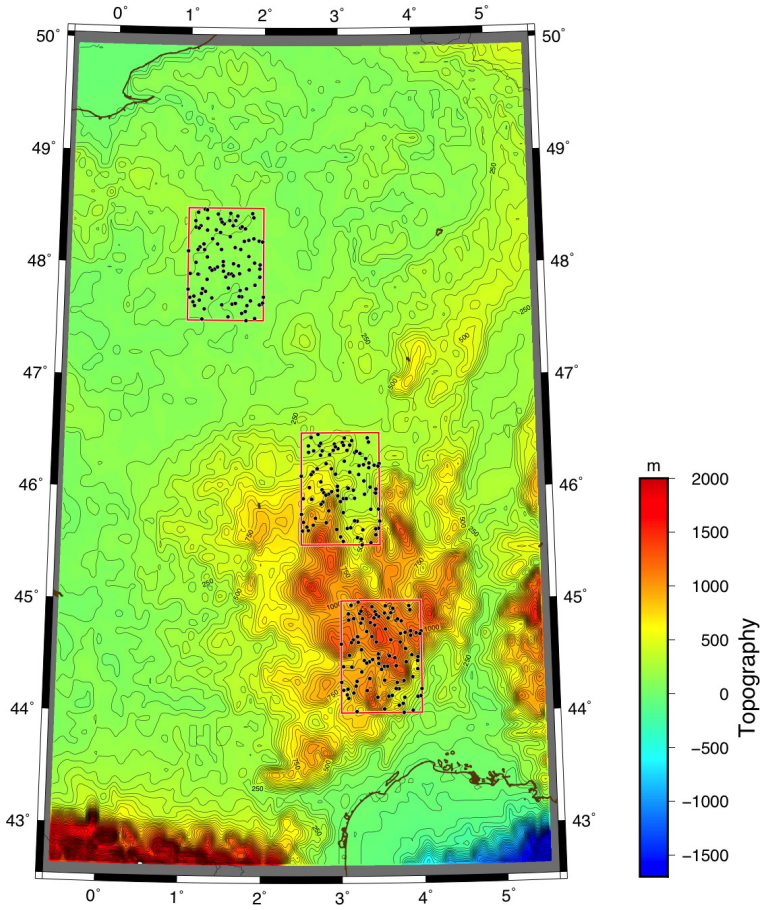

Figure 2: The topography around the test zones, red rectangles, in France

	Zone(1)	Zone(2)	Zone(3)
Lat(°)	47.50-48.49	45.51-46.49	44.00-44.98
Long(°)	1.00-1.99	2.50-3.49	3.00-3.99
Hmin(m)	84.00	247.00	142.50
Hmax(m)	242.00	1379.70	1394.40
Hmean(m)	131.96	523.70	958.54
Rms(m)	134.24	576.22	989.43
Std(m)	24.47	240.43	245.39

Table 1: Statistics of heights in test areas derived from the digital model ETOPO5 [1]

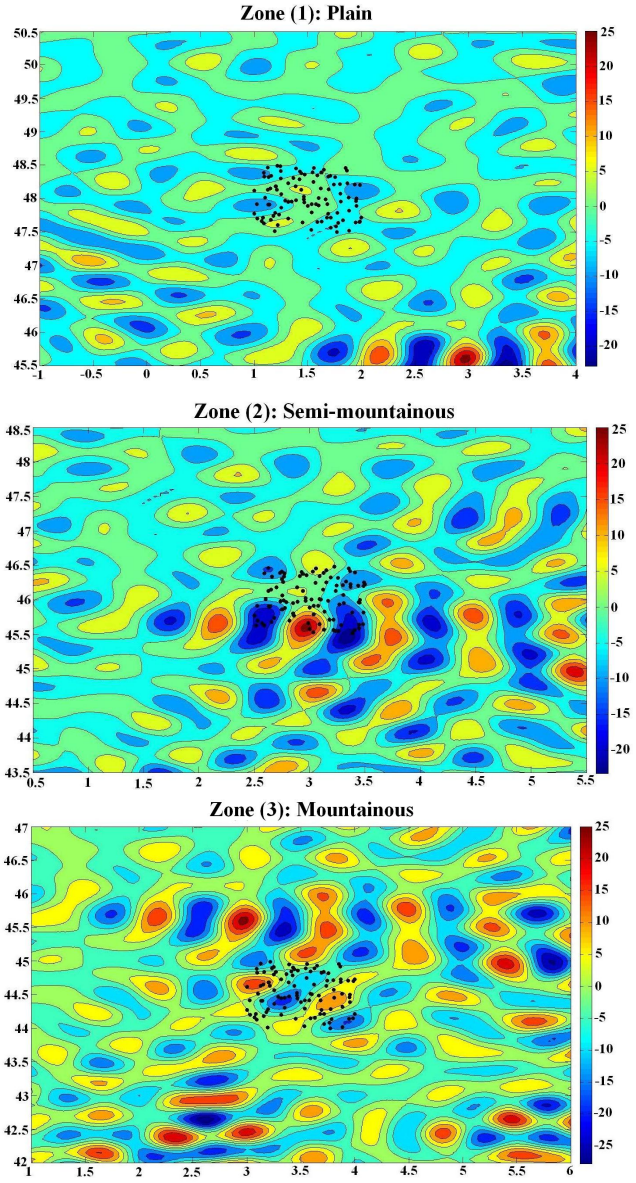

Figure 3: Residual gravity anomaly of the test zones in France for wavelength bands between degree 600 and 800. Radius of Stokes' integration= 2°. Gravity anomaly grid resolution = 0.050°. The black dots represent the test points in each area.

$\triangle g_{res}$	Zone(1)	Zone(2)	Zone(3)
Min(mgal)	-22.8	-23.33	-27.92
Max (mgal)	26.86	26.86	26.86
Mean(mgal)	-0.002	-0.003	-0.074
Std (mgal)	4.63	6.12	7.34

Table 2: Statistics of Residual gravity anomaly in test areas derived from the EGM2008 model [6]

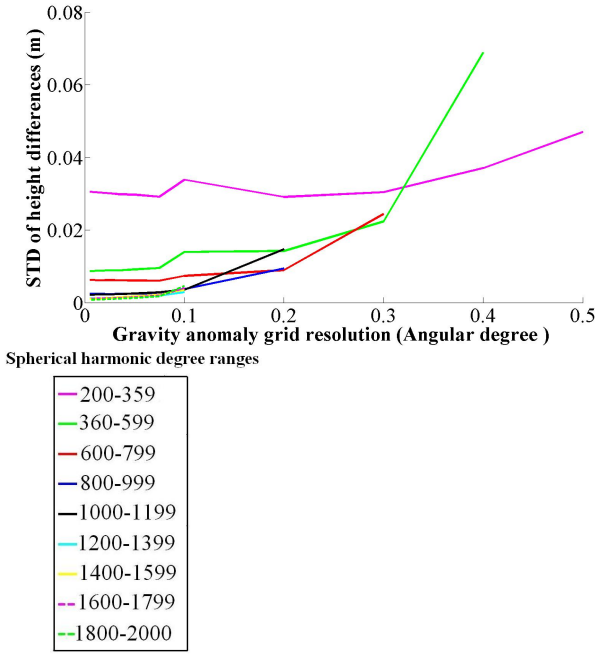

Figure 4: Accuracy of the geoid heights in meters computed using the standard Stokes' kernel as a function of the gravity anomaly grid resolution averaged on the three test areas. Integration radius=2°. Colors correspond to different frequency ranges(see legend)

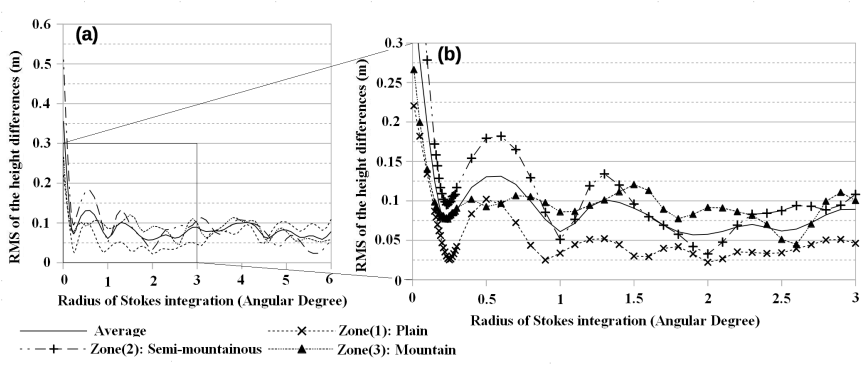

Figure 5: Error ϵ in m (Equation 8) as function of the integration radius in angular degrees for a geopotential model at degree 199. Left (a): evolution up to 6°; right (b): zoom of (a) on small integration radii. Curves correspond to different test areas (see legend)

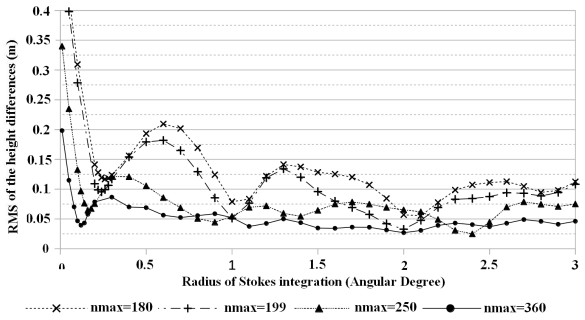

Figure 6: Error ϵ in m (Equation 8) as function of the integration radius in angular degrees for the semi-mountainous test area (Zone 2). Curves correspond to different values of maximum degree n_{max} of the EGM2008 geopotential model (see legend)

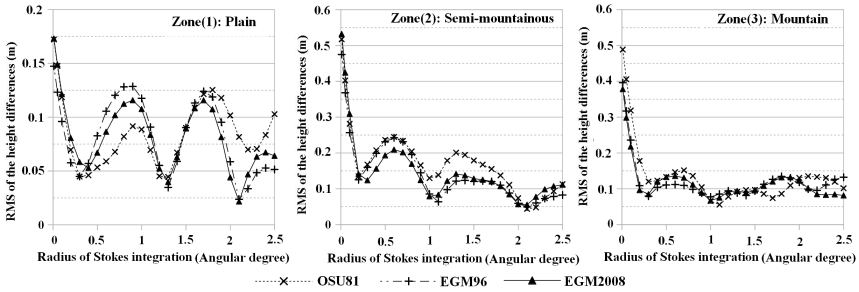

Figure 7: Error ϵ in m (Equation 8) as function of the integration radius in angular degrees for the 3 test areas. Left: plain; center: semi-mountainous; right: mountain. Curves correspond to the use of different geopotential models for the computation of W_M as defined in section 3.2 (see legend)

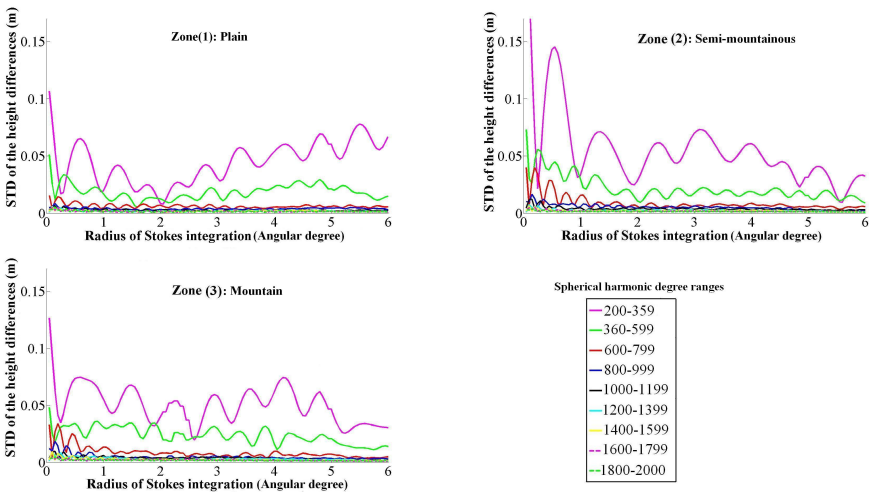

Figure 8: Accuracy of the geoid heights in meters computed using the standard Stokes' kernel as a function of the integration radius in three test zones. Gravity anomaly grid resolution =0.05°. Colors correspond to different frequency ranges(see legend)

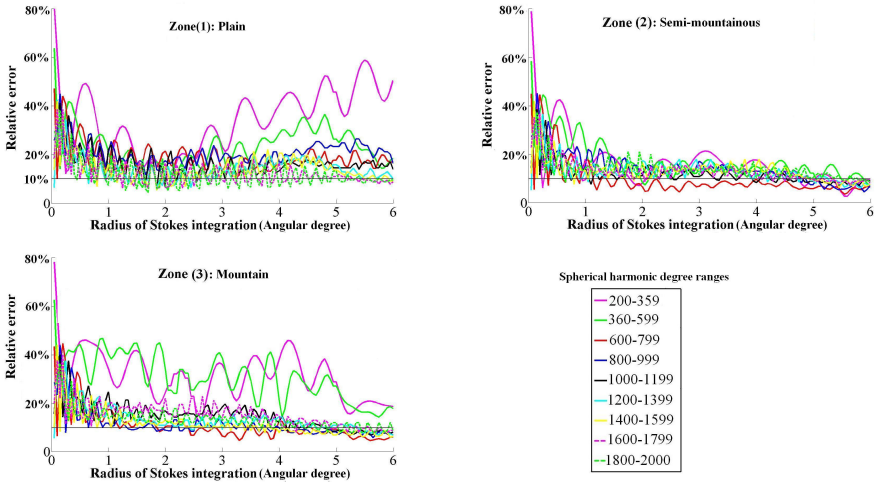

Figure 9: Relative accuracy of the geoid heights computed using the standard Stokes' kernel as a function of the integration radius in three test zones. Gravity anomaly grid resolution =0.05°.Colors correspond to different frequency ranges(see legend)

References

[1] Digital Relief of the Surface of the Earth. Data Announcement 88-MGG-02, NOAA, National Geophysical Data Center, Boulder, Colorado, 1988.

[2] H. Duquenne. A New Solution for the Quasigeoid in France QGF98. In *Proceedings of the 2nd Continental Workshop on the Geoid in Europe, Budapest*, volume 98 of *Finnish Geodetic Institut reports*, pages 251–255, March 1998.

[3] Henri Duquenne. A Data Set to Test Geoid Computation Methods. *Harita Dergisi*, (18):61–65, 2007. Proc. 1st international symposium of the International Gravity Field Service 'Gravity field of the Earth', Istanbul, Turkey, Aug. 2006.

[4] A. Ellmann. *The Geoid for the Baltic Countries Determined by the Least Squares Modification of Stokes Formula*. PhD thesis, Royal Institute of Technology (KTH), Stockholm, 2004. Doctoral Dissertation in Geodesy No.1061.

[5] O. Esan. *Spectral Analysis of Gravity Field Data and Errors in View of Sub-Decimeter Geoid Determination in Canada*. PhD thesis, The University of Calgary, Calgary, Alberta, Canada, 2000.

[6] M. Eshagh. A Strategy Towards an EGM08-based Fennoscandian Geoid Model. *Journal of Applied Geophysics*, 87:53–59, 2012.

[7] W.E. Featherstone. Tests of Two Forms of Stokes's Integral Using a Synthetic Gravity Field Based on Spherical Harmonics. In ErikW. Grafarend, FriedrichW. Krumm, and VolkerS. Schwarze, editors, *Geodesy-The Challenge of the 3rd Millennium*, pages 163–171. Springer Berlin Heidelberg, 2003.

[8] W.E. Featherstone, J.F. Kirby, C. Hirt, M.S. Filmer, S.J. Claessens, N.J. Brown, G. Hu, and G.M. Johnston. The AUSGeoid09 model of the Australian Height Datum. *Journal of Geodesy*, 85(3):133–150, 2011.

[9] J. Flury. Short-Wavelength Spectral Properties of the Gravity Field from a Range of Regional Data Sets. *Journal of Geodesy*, 79(10-11):624–640, 2006.

[10] R. Forsberg. Modelling the Fine Structure of the Geoid: Methods, Data Requirements and Some Results. *Surveys in Geophysics*, 14:403–418, 1993.

[11] W.A. Heiskanen and H. Moritz. *Physical geodesy*, volume 86. Springer-Verlag, 1967.

[12] M.B. Higgins, R. Forsberg, and A.H.W. Kearsley. The Effects of Varying Cap Sizes on Geoid Computations: Experiences with FFT and Ring Integration. In Rene Forsberg, Martine Feissel, and Reinhard Dietrich, editors,

Geodesy on the Move, volume 119 of *International Association of Geodesy Symposia*, pages 201–206. Springer Berlin Heidelberg, 1998.

[13] C. Hwang, C.G. Wang, and Y.S. Hsiao. Terrain Correction Computation Using Gaussian Quadrature. *Computers and Geosciences*, 29:1259–1268, 2003.

[14] A.H.W Kearsley. Data Requirements for Determining Precise Relative Geoid Heights from Gravimetry. *Journal of Geophysical Research*, 91(B9):9193–9201, Aug 1986.

[15] A.H.W Kearsley. The Determination of Precise Geoid Height Differences Using Ring Integration. *Bollettino Di Geodesia E Scienze Affini*, (2):151–174, 1986.

[16] A.H.W Kearsley. Tests on the Recovery of Precise Geoid Height Differences from Gravimetry. *Journal of Geophysical Research*, 93(B6):6559–6570, June 1988.

[17] A. KiliCoglu, C. A. Diren, H. Yildiz, M. Bolme, B. AAktug, M. Simav, and O. Lenk. Regional Gravimetric Quasi-Geoid Model and Transformation Surface to National Height System for Turkey (THG-09). *Studia Geophysica et Geodaetica*, 55(4):557–578, 2011.

[18] T. Krarup. A Contribution to the Mathematical Foundation of Physical Geodesy. In Kai Borre, editor, *Mathematical Foundation of Geodesy*, pages 29–90. Springer Berlin Heidelberg, 2006.

[19] J. Krynski and A. Lyszkowicz. Centimetre Quasigeoid Modelling in Poland using Heterogeneous Data. In *Gravity Field of the Earth*, volume 18 of *IAG Proceedings of the 1st International Symposium of the International Gravity Field Service (IGFS)*, pages 37–42. Istanbul, Turkey, 2006.

[20] F. G. Lemoine, S. C. Kenyon, J. K. Factor, R.G. Trimmer, N. K. Pavlis, D. S. Chinn, C. M. Cox, S. M. Klosko, S. B. Luthcke, M. H. Torrence, Y. M. Wang, R. G. Williamson, E. C. Pavlis, R. H. Rapp, and T. R. Olson. The Development of the Joint NASA GSFC and NIMA Geopotential Model EGM96. Technical Report TP-1998-206861, NASA Goddard Space Flight Center, Greenbelt, Maryland, 20771 USA, July 1998.

[21] H.T Moritz. *Advanced Physical Geodesy*. Sammlung Wichmann: Neue Folge, Buchreihe. Wichmann, 1980.

[22] I. Panet, Y. Kuroishi, and M. Holschneider. Wavelet Modelling of the Gravity Field by Domain Decomposition Methods: An Example Over Japan. *Geophysical Journal International*, 184:203–219, 2011.

[23] Nikolaos K. Pavlis, Simon A. Holmes, Steve C. Kenyon, and John K. Factor. The Development and Evaluation of the Earth Gravitational Model 2008 (EGM2008). *Journal of Geophysical Research: Solid Earth*, 117(B4), Apr. 2012.

[24] R.H. Rapp. The Earth's Gravity Field to Degree and Order 180 Using Seasat Altimeter Data, Terrestrial Ggravity Data and other Data. Technical Report 32, Dep. of Geod. Sci. and Surv., Ohio State University, Colombus, 1981.

[25] L.E. Sjoberg. A General Model for Modifying Stokes's Formula and its Least-Squares Solution. *Journal of Geodesy*, 77(7-8):459–464, 2003.

[26] N. Srinivas, V.M. Tiwari, J.S. Tarial, S. Prajapti, A.E. Meshram, B. Singh, and B. Nagarajan. Gravimetric Geoid of a Part of South India and its Comparison with Global Geopotential Models and GPS-Levelling Data. *Journal of Earth System Science*, 121(4):1025–1032, 2012.

[27] G.G Stokes. *On the Variation of Gravity at the Surface of the Earth.* Trans. Cambridge Philosophical Society VIII, 1849.

[28] R.Forsberg & C.C Tscherning. *Geodetic Gravity Field Modelling Programs*, 2003.

[29] P. Valty and H. Duquenne. Quasi-Geoid of New Caledonia: Computation, Results and Analysis. In Stelios P. Mertikas, editor, *Gravity, Geoid and Earth Observation*, volume 135 of *International Association of Geodesy Symposia*, pages 427–435. Springer Berlin Heidelberg, 2010.

[30] P. Valty, H. Duquenne, and I. Panet. Auvergne Dataset: Testing Several Geoid Computation Methods. In *Geodesy for Planet Earth*, volume 136 of *International Association of Geodesy Symposia*, pages 465–472. Springer Berlin Heidelberg, 2012.

[31] H. Yildiz, R. Forsberg, J. Agren, and L.E. Tscherning, C. C.and Sjoberg. Comparison of Remove-Compute-Restore and Least Squares Modification of Stokes' Formula Techniques to Quasi-geoid Determination over the Auvergne Test area. *Journal of Geodetic Science*, 2:53–64, 2011.